

Cascading GEMM: High Precision from Low Precision

Devangi Parikh*, Robert van de Geijn† and Greg Henry‡

March 9, 2023

Abstract

This paper lays out insights and opportunities for implementing higher-precision matrix-matrix multiplication (GEMM) from (in terms of) lower-precision high-performance GEMM. The driving case study approximates double-double precision (FP64x2) GEMM in terms of double precision (FP64) GEMM, leveraging how the BLAS-like Library Instantiation Software (BLIS) framework refactors the Goto Algorithm. With this, it is shown how approximate FP64x2 GEMM accuracy can be cast in terms of ten “cascading” FP64 GEMMs. Promising results from preliminary performance and accuracy experiments are reported. The demonstrated techniques open up new research directions for more general cascading of higher-precision computation in terms of lower-precision computation for GEMM-like functionality.

1 Introduction

The advent of processors with new floating point precisions, including various low precision formats (like half-precision), has raised the question of how to leverage the higher performance of low-precision arithmetic into high performance for high-precision arithmetic [1, 11, 13]. In this paper, we gain insight into possibilities by primarily focusing on one end of the spectrum: the implementation of double-double precision (FP64x2) matrix-matrix multiplication (GEMM) in terms of high-performance double precision (FP64) GEMM. This is an interesting study because currently FP64x2 is not supported by contemporary CPUs in hardware yet is of interest to some applications [9]. We then use this case study to discuss a range of new directions that can be explored along the same lines (e.g., casting single precision in terms of half precision).

Our community demands high performance from its GEMM implementations [10]. This is for good reasons: in one form or another, much computation in scientific computing and, more recently, machine learning can be cast in terms of a GEMM-like computation. Thus, understanding high-performing GEMM contributes to high-performing higher-level functionality. For this reason, proposing new techniques should be accompanied by a demonstration of how to achieve performance.

A current framework for effectively implementing GEMM functionality is the BLAS-like Library Instantiation Software (BLIS) [21, 27, 31, 32, 33]. Not only does BLIS support high performance that is portable to a variety of contemporary CPUs, but it also allows GEMM-like functionality to be quickly realized. Key to this is how the framework isolates architecture-specific code and parameters, and how submatrices are packed for data locality. The principles that underly BLIS have been exploited in a number of situations, including for tensor contraction [22], practical Strassen’s algorithms [16, 17], k-Nearest Neighbor computations [35], complex GEMM in terms of real GEMM [29], and mixed-precision/mixed-domain GEMM [30]. The present work similarly exploits those techniques.

This paper makes the following contributions:

*Department of Computer Science and Oden Institute, The University of Texas at Austin, Austin, TX 78712, dnp@cs.utexas.edu

†Department of Computer Science and Oden Institute, The University of Texas at Austin, Austin, TX 78712, rvdg@cs.utexas.edu

‡2111 NE 25th Avenue, Hillsboro OR 97124, greg.henry@intel.com

- A strategy for cascading FP64x2 matrices into multiple FP64 matrices that enables the estimating of FP64x2 GEMM with ten FP64 GEMMs.
- A prototype implementation that demonstrates how to make the proposed scheme practical, by which we mean that it:
 - achieves high performance and high accuracy,
 - requires similar workspace to what is already used in a high performance FP64 GEMM implementation,
 - leverages existing kernels for FP64 GEMM for portable high performance, and
 - performs all higher-order $O(n^3)$ work with FP64 arithmetic only (no double-double or quadruple precision work and most of the $O(n^2)$ work done also in FP64 arithmetic only.)
- A discussion of new opportunities, including:
 - how cascading can more generally support high precision GEMM in term of lower precision GEMM,
 - opportunities for leveraging GPUs,
 - the need for in-depth numerical analysis,
 - benefits of scaling/balancing nmethods,
 - the potential of hardware support for cascading, and
 - how to support other level-3 BLAS functionality.

This not only advances the understanding of how to implement FP64x2 GEMM in terms of FP64 GEMM, but it suggests many new directions of research.

Since many symbols are used in this paper, we provide a glossary in Figure 1.

2 Background

The use of single precision (FP32) and double precision (FP64) storage and arithmetic in GEMM is well understood and usually supported in hardware. A fused-multiply-accumulate (FMA) in FP64 typically requires twice the time of a FP32 FMA. More recently, variants on half precision like bfloat16 have become of interest and are also more and more supported in hardware [5]. Conceptually, a straight forward precision beyond FP64 is quad precision (FP128), which uses a mantissa of 113 (112 stored) bits and exponent of 15 bits compared to a mantissa of 53 (52 stored) and exponent of 11 bits for FP64. Hardware support for quad precision is only found on a few processors, largely because the hardware area to support fast FP arithmetic grows quadratically with the mantissa size. Instead simulating FP128 arithmetic in software on the FMA level requires approximately two orders of magnitude more time than a FP64 FMA.

A compromise is double-double (FP64x2) precision, which stores an extended precision number in two FP64 numbers, splitting the mantissa among the two, but providing no greater exponent range. The benefit is that now 106 bits are available for the mantissa, and casting a FP64x2 FMA in terms of FP64 FMAs is simpler and requires less computation time [2] than FP128 when both are implemented in software. The problem is that it is still time intensive, with a FP64x2 FMA implemented in software still requiring approximately 30-50 times more time than a hardware FP64 FMA. An early attempt at supporting such extended precision for BLAS functionality was the reference XBLAS [20, 34], which make no attempt at optimizing performance.

One problem with early papers on the topic of FP64x2 is that they measure performance by counting flops rather than FMAs. Extrapolating from the cost of a FP64 dot product of size n requiring roughly n FP64 multiplies and n FP64 adds, many higher-accuracy dot product strategies would, for example, state an algorithm that requires $20n$ FP64 flops as being $10\times$ more overhead than FP64 dot products. However, a careful analysis of many of these high precision kernels shows a huge bias toward adds and subtracts over multiplies. This gap is further widened on machines that support FP64 FMAs (nearly all of them), because emulating FP64x2 multiplication only requires 1 FMA and 1 multiply instruction, while FP64x2 addition requires approximately 10 or more add/subtract instructions that are dependent on each other. Therefore, a FP64x2 multiplication is significantly simpler than FP64x2 addition/subtraction. It's better

Symbol	Comment
$\hat{}$	Quantity/variable associated with FP64x2 number.
$\tilde{}$	Quantity/variable associated with cascaded number
A, B, C	Matrices (upper case Roman letters).
χ, ψ	Scalars (lower case Greek letters)
$\alpha_{i,j}$	(i, j) entry of A .
$\beta_{i,j}$	(i, j) entry of B .
x, y	(Column) vectors (lower case Roman letters).
c_0, c_1, c_2	Number of digits in chunks 0, 1, 2. $c_i = D_{i+1} - D_i$.
D	# binary digits in mantissa of a FP64. $D = 53$ for FP64.
D_0, D_1, D_2	Boundaries between digit ranges for chunks of the cascaded number.
D_A	$= \text{diag}(\max_j \alpha_{0,j} , \max_j \alpha_{1,j} , \dots)$.
D_B	$= \text{diag}(\max_i \beta_{i,0} , \max_j \alpha_{i,1} , \dots)$.
$\delta\chi, \delta x, \delta y, \Delta A, \Delta B$	Error in χ, x, y, A, B .
ϵ_{mach}	Machine epsilon for FP64. $\epsilon_{\text{mach}} = 2^{-D} = 2^{-53}$.
$\hat{\epsilon}_{\text{mach}}$	Machine epsilon for FP64x2. $\hat{\epsilon}_{\text{mach}} = 2^{-2D} = 2^{-106}$.
$\tilde{\epsilon}_{\text{mach}}$	Machine epsilon for cascaded number. $\tilde{\epsilon}_{\text{mach}} = 2^{-(D_2+D)} = 2^{-117}$.
FP64	Double (64 bit) floating point.
FP64x2	Double-double floating point.
σ	Scaling factors for x, A .
Σ	Diagonal matrix of scaling factors for A .
τ	Scaling factors for x, y, A, B .
T	Diagonal matrix of scaling factors for B .
$\sigma_1, \sigma_2, \sigma_2$	Scaling factors for bins 0, 1, 2.

Figure 1: Glossary. Text in blue is for the example of FP64x2, but can be generalized/modified for other precisions.

to have an algorithm with n FMAs than one with $1.5n$ adds, even though technically the latter incurs fewer flops.

Another avenue of earlier works focus on the idea of “generating a more accurate sum” [26] or “dot-product” [3, 8, 24]. The idea is that if a dot product algorithm produces a more accurate result, it can be useful in computing a more accurate GEMM. For example, [25] discusses how to split a higher precision GEMM via error-free transformations that are not dependent on conditionals, exploiting only regular floating-point add, subtract and multiplication vector instructions. Also, in [13] it is discussed how to cast a FP32 FMA in terms of three bfloat16 FMAs, which is the concept applied in the present work to yield what we call cascading GEMM matrices.

An important distinction to note is that, in most previous work that deals with higher accuracy GEMM (or dot products) using lower precision computation, the input matrices A and B are stored in the lower precision. For instance, [23] explores the use of low precision tensor cores on Nvidia GPUs to

do cascading matrices with whatever low precision the tensor core supports. Similarly, in [11] it is also shown how to perform multi-precision GEMM. Both extend the ideas in [13]. In addition, [25] discusses computing AB in higher accuracy, when A and B are in FP64. This case requires about one-half to one-quarter of the work involved in computing the more general case when A and B are in FP64x2. They distinguish between two cases: one that exploits sparsity and skips some GEMM computation, for which they report 13× slowdown over dgemm, and one that ignores sparsity gets 18× slowdown. In contrast, in this paper, we consider the case where A and B , as well as the computation AB is done in FP64 accuracy. We propose an algorithm that requires 2-4× as many computations, and yet still show similar or better performance than the sparse case cited in [25].

Early work on breaking up higher precision GEMM in terms of lower precision GEMM was given in [13] and extended in [11]. We view present paper as encompassing much of that work, although explained using the example of cascading FP64x2 in terms of FP64 matrix multiplication.

3 Cascading

We illustrate the fundamental ideas with a case study that shows how to cascade FP64x2 GEMM into FP64 GEMMs. How the techniques extend will be discussed later.

3.1 FP64 and FP64x2 numbers

A normalized FP64 number, χ , consists of a sign, a mantissa, and an exponent:

$$\chi = \pm \cdot \beta_0 \cdots \beta_{D-1} \times 2^e = \pm \left(\beta_0 \times 2^{-1} + \beta_1 \times 2^{-2} + \cdots + \beta_{D-1} \times 2^{-D} \right) \times 2^e,$$

where $\beta_0 = 1$. A typical D equals 53 and for that reason that integer will frequently appear in our discussions.

A double-double floating point number (FP64x2), $\hat{\chi}$, increases the size of the mantissa by using two normalized FP64 numbers:

$$\hat{\chi} = \chi_0 + \chi_1 \times 2^{-D} = \underbrace{\pm \cdot \beta_0 \cdots \beta_{D-1} \times 2^e}_{\chi_{hi}} + \underbrace{\pm \cdot \beta_{D+G} \cdots \beta_{2D+G-1} \times 2^{e-G}}_{\chi_{lo}} \times 2^{-D}. \quad (1)$$

Here,

- We add a $\hat{\cdot}$ to denote a FP64x2 variable.
- There are no overlapped (ranges of) bits in χ_{hi} and χ_{lo} ,
- $G \geq 0$ captures that there could be leading zeroes (a *gap*) right where the split of the FP64x2 number happens.

This gap allows more accuracy to be stored in a FP64x2 than a $2D$ bit mantissa would, if one is lucky where zero bits occur. However, one can obviously not count on that extra accuracy and hence in our discussion we will mostly assume $G = 0$ and will refer to it as a *lucky gap* to emphasize that it cannot be counted on.

3.2 Cascading scalars and scalar multiplication

Consider the FP64x2 number discussed in Section 3.1, $\hat{\chi} = \chi_{hi} + \chi_{lo} \times 2^{-D}$ and a second FP64x2 number $\hat{\psi} = \psi_{hi} + \psi_{lo} \times 2^{-D}$. Then

$$\hat{\chi}\hat{\psi} = \chi_{hi}\psi_{hi} + \chi_{hi}\psi_{lo} \times 2^{-D} + \chi_{lo}\psi_{hi} \times 2^{-D} + \chi_{lo}\psi_{lo} \times 2^{-2D}.$$

This seems to illustrate how a single FP64x2 multiplication can be broken down into four FP64 multiplications, some shifts of the exponents, and three FP64x2 additions. The problem is that each of the four terms may incur error when computed in FP64, including in the product of the highest order term, $\chi_0\psi_0$, because a FP64 multiplication can produce $2D$ bits in the mantissa of the result which are stored back into a D bit FP64 before adding the terms together.

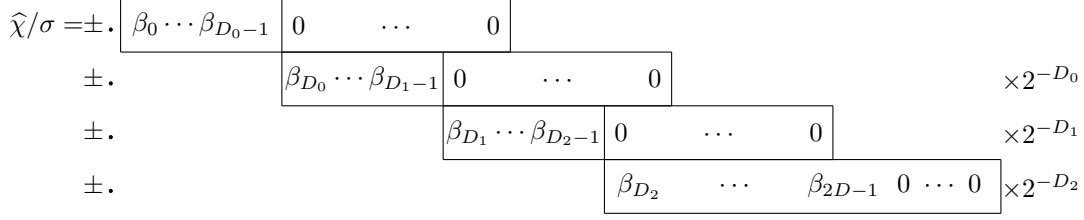


Figure 2: Illustration of how FP64x2 number $\hat{\chi}$ is cascaded into four FP64 chunks. Here we assume that we start with a normalized number so that $\beta_0 = 1$. If $D_i \leq D$ for $i = 0, 1, 2$, then this also illustrates that additional precision can be stored in the cascaded number, which can improve accuracy when the cascaded representation is used for intermediary accumulation.

One can try to overcome these multiplication inaccuracies by approximating

$$\hat{\chi} \approx \chi_0 + \chi_1 \times 2^{-D_0},$$

where $\chi_0 = \pm \cdot \beta_0 \beta_1 \cdots \beta_{D_0-1} \times 2^e$ and $\chi_1 \approx \pm \cdot \beta_{D_0} \cdots \beta_{D_0+D-1} \times 2^e$. Now, if $D_0 \leq D/2$ then $\chi_0 \psi_0$ is computed exactly in FP64 arithmetic since the result has at most D bits in the mantissa. However, one would expect a loss in accuracy since digits beyond β_{D_0+D-1} vanish in the conversion (unless there is a *lucky gap*).

With this introduction, we instead consider cascading (splitting) a scaled FP64x2, $\hat{\chi}$, into four FP64s (chunks). We start with

$$\hat{\chi}/\sigma = \pm \cdot \beta_0 \cdots \beta_{D_0-1} \beta_{D_0} \cdots \beta_{D_1-1} \beta_{D_1} \cdots \beta_{D_2-1} \beta_{D_2} \cdots \beta_{D_2+D-1} \beta_{D_2+D} \cdots,$$

where σ is a power of two that has the property that β_0 may or may not equal a zero bit. In other words, $\sigma \leq 2^e$, where e is the exponent that occurs in (1). We can now “cascade” this scaled FP64x2 number into four FP64s:

$$\hat{\chi}/\sigma \approx \pm \cdot \boxed{\beta_0 \cdots \beta_{D_0-1} \quad \beta_{D_0} \cdots \beta_{D_1-1} \quad \beta_{D_1} \cdots \beta_{D_2-1} \quad \beta_{D_2} \cdots \beta_{D_2+D-1}},$$

and represent (approximately) $\hat{\chi}/\sigma$ in terms of four FP64s:

$$\begin{aligned} \hat{\chi}/\sigma \approx & \underbrace{\pm \cdot \beta_0 \cdots \beta_{D_0-1}}_{\chi_0} + \underbrace{\pm \cdot \beta_{D_0} \cdots \beta_{D_1-1}}_{\chi_1} \times \underbrace{2^{-D_0}}_{\sigma_1} \\ & + \underbrace{\pm \cdot \beta_{D_1} \cdots \beta_{D_2-1}}_{\chi_2} \times \underbrace{2^{-D_1}}_{\sigma_2} + \underbrace{\pm \cdot \beta_{D_2} \cdots \beta_{D_2+D-1}}_{\chi_3} \times \underbrace{2^{-D_2}}_{\sigma_3}. \end{aligned}$$

This is also illustrated in Figure 2. More concisely

$$\hat{\chi} \approx \sigma (\chi_0 + \sigma_1 \chi_1 + \sigma_2 \chi_2 + \sigma_3 \chi_3).$$

If $\beta_0 = 1$, $D_0 + D_1 + D_2 + D > 2D$, and there is no lucky gap in the FP64x2 representation, then the cascaded representation can store more digits than FP64x2. Even more precision may result if there is a gap at the beginning of χ_3 , but that cannot be counted on. In other words, if the cascaded number holds the result of other computations, it may hold extra precision in the trailing zeroes of χ_3 . We consider the existence of a cascading split for any FP64x2 number to be self-evident.

If we similarly cascade a second FP64x2 number, $\hat{\psi}$:

$$\hat{\psi} \approx \tau (\psi_0 + \sigma_1 \psi_1 + \sigma_2 \psi_2 + \sigma_3 \psi_3),$$

then the product of these two scalars equals, approximately,

$$\begin{aligned}
\widehat{\chi}\widehat{\psi} \approx \sigma\tau(& \underbrace{\chi_0\psi_0}_{\text{bin 0}} + \underbrace{\sigma_1\chi_0\psi_1}_{\text{bin 1}} + \underbrace{\sigma_2\chi_0\psi_2}_{\text{bin 2}} + \underbrace{\sigma_3\chi_0\psi_3}_{\text{bin 3}} \\
& + \underbrace{\sigma_1\chi_1\psi_0}_{\text{bin 1}} + \underbrace{\sigma_1^2\chi_1\psi_1}_{\text{bin 2}} + \underbrace{\sigma_1\sigma_2\chi_1\psi_2}_{\text{bin 3}} + \underbrace{\sigma_1\sigma_3\chi_1\psi_3}_{\text{bin 4}} + \\
& + \underbrace{\sigma_2\chi_2\psi_0}_{\text{bin 2}} + \underbrace{\sigma_2\sigma_1\chi_2\psi_1}_{\text{bin 3}} + \underbrace{\sigma_2^2\psi_2}_{\text{bin 4}} + \underbrace{\sigma_2\sigma_3\chi_2\psi_3}_{\text{bin 5}} + \\
& + \underbrace{\sigma_3\chi_3\psi_0}_{\text{bin 3}} + \underbrace{\sigma_3\sigma_1\chi_3\psi_1}_{\text{bin 4}} + \underbrace{\sigma_3\sigma_2\chi_3\psi_2}_{\text{bin 5}} + \underbrace{\sigma_3^2\chi_3\psi_3}_{\text{bin 6}}).
\end{aligned}$$

Notice that

$$\begin{aligned}
\text{bin 1:} \quad & \sigma_1 = 2^{-D_0} \\
\text{bin 2:} \quad & \sigma_1^2 \approx \sigma_2 = 2^{-D_1} \\
\text{bin 3:} \quad & \sigma_1\sigma_2 \approx \sigma_3 = 2^{-D_2} \\
\text{bin 4:} \quad & \sigma_2^2 \approx \sigma_1\sigma_3 \ll 2^{-D_2} \\
\text{bin 5:} \quad & \sigma_2\sigma_3 \ll 2^{-D_2} \\
\text{bin 6:} \quad & \sigma_3^2 \ll 2^{-D_2}.
\end{aligned}$$

The ‘‘approximate’’ here means that they are equal plus or minus one, if the sizes of chunks are chosen appropriately. If D_0 , D_1 , and D_2 are chosen carefully¹, the first three bins can be computed and stored exactly in FP64.

Thus, the process becomes:

1. Transform $\widehat{\chi}$ and $\widehat{\psi}$ into cascaded representation.
2. Compute within the bins in FP64 arithmetic.
3. Add within and across the bins in appropriate precision.

We note that accumulating the contributions across a few of the higher-order bins (bin 0, bin 1 and bin 2.) must be in higher than double precision (in FP64x2 arithmetic or some compensated two-sum algorithm [7]) and the rest can be summed in FP64.

Let us analyze the error introduced when cascading a FP64x2:

$$\widehat{\chi} = \sigma(\chi_0 + \chi_1\sigma_1 + \chi_2\sigma_2 + \chi_3\sigma_3 + \delta\chi),$$

where $|\delta\chi| \leq 2^{-(D_0+D_1+D_2+D)}$ if rounding is used to create the fourth chunk. In $\delta\chi$ the δ touches the χ to indicate this is one symbol to represent the error term following the conventions in [4]. This means that

$$\widehat{\chi} = \sigma(\chi_0 + \chi_1\sigma_1 + \chi_2\sigma_2 + \chi_3\sigma_3) + \sigma\delta\chi,$$

where $|\sigma\delta\chi| \leq 2^{-(D_2+D)}\sigma$. This bound is actually pessimistic, since the last chunk, χ_3 will hold a full FP64 number and hence even if $\chi_0 = \chi_1 = \chi_2 = 0$, the last chunk holds a FP64 approximation of the FP64x2 number. This allows us to refine the bound to

$$|\delta\chi\sigma| \leq \min(2^{-(D_2+D)}\sigma, \epsilon_{\text{mach}}\widehat{\chi}), \quad (2)$$

where $\epsilon_{\text{mach}} = 2^{-D}$ and $\widetilde{\epsilon}_{\text{mach}} = 2^{-(D_2+D)}$ are the *machine epsilon* for an FP64 and a cascaded number, respectively.

3.3 Cascading vectors and dot products

On our way to understanding the properties of using cascading arithmetic within a GEMM, we propose how to cascade vectors and examine a dot product with such vectors.

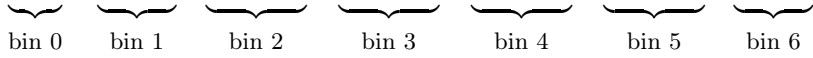
¹How to choose these parameters will become clear shortly

Let \hat{x} and \hat{y} be vectors of size k with FP64x2 numbers as their entries. We wish to compute $\alpha = \hat{x}^T \hat{y}$. We cascade each of the vectors:

$$\begin{aligned}\hat{x} &\approx \sigma (x_0 + \sigma_1 x_1 + \sigma_2 x_2 + \sigma_3 x_3) \\ \hat{y} &\approx \tau (y_0 + \sigma_1 y_1 + \sigma_2 y_2 + \sigma_3 y_3)\end{aligned}$$

so that

$$\begin{aligned}\hat{x}^T \hat{y} \approx \sigma \tau (& x_0^T y_0 + \sigma_1 x_0^T y_1 + \sigma_2 x_0^T y_2 + \sigma_3 x_0^T y_3 \\ & + \sigma_1 x_1^T y_0 + \sigma_1^2 x_1^T y_1 + \sigma_1 \sigma_2 x_1^T y_2 + \sigma_1 \sigma_3 x_1^T y_3 + \\ & + \sigma_2 x_2^T y_0 + \sigma_2 \sigma_1 x_2^T y_1 + \sigma_2^2 x_2^T y_2 + \sigma_2 \sigma_3 x_2^T y_3 + \\ & + \sigma_3 x_3^T y_0 + \sigma_3 \sigma_1 x_3^T y_1 + \sigma_3 \sigma_2 x_3^T y_2 + \sigma_3^2 x_3^T y_3).\end{aligned}\quad (3)$$



Now examine under what circumstances chunks $i, j \in \{0, 1, 2\}$ of $x_i^T y_j$ are guaranteed to be computed exactly. Consider that

$$x_i^T y_j = \chi_{0,i} \psi_{0,j} + \chi_{1,i} \psi_{1,j} + \dots + \chi_{k-1,i} \psi_{k-1,j},$$

where $\chi_{p,i}$ is the p -th element of the cascaded vector x_i . In order to compute each $\chi_{p,i} \psi_{p,j}$ exactly and add these results together to be exact, we observe that:

- Each element in x must be chunked into the same ranges. This means
 - Finding the element with largest magnitude and divide all terms in that dot product by the smallest power of two greater than that value (normalizing everything in the vector.) This tells us how to choose σ and τ .
 - Chunking all other elements conformally, by which we mean that corresponding chunks are taken from the same range.

Observe that elements other than the one with largest magnitude may have leading zeroes, including in their most significant chunk².

- Adding k contributions from the terms in the dot product may yield a result with $\lceil \log_2 k \rceil$ additional binary digits that must be tracked. Adding the products within a bin may magnify the number of bits further.

Assume that x and y are each chunked so that $c_i = D_{i+1} - D_i$ for $i \in \{0, 1, 2\}$ and $c_3 \leq 2D - D_2$, and take $k = 256$ so that $\log_2 k = 8$ as an example³. Then

- To ensure that bin 0 is computed in full accuracy, we constrain c_0 such that $2c_0 + \log_2 k \leq 53$. This suggests that $c_0 \leq (53 - 8)/2$. Thus, chunk 0 can accommodate $c_0 = 22$ bits.
- To ensure that bins 1 and 2 are computed in full accuracy, we must constrain c_1 such that both $c_0 + c_1 + \log_2 k + \lceil \log_2 2 \rceil \leq 53$ and $2c_1 + \log_2 k + \lceil \log_2 3 \rceil \leq 53$. The 2 and 3 come from the number of terms that need to be added in bin 1 and bin 2 respectively. This implies that chunk 1 can accommodate only $c_1 = 21$ bits.
- To ensure that bin 2 is computed in full accuracy, we constrain c_2 such that $c_0 + c_2 + \log_2 k + \lceil \log_2 4 \rceil \leq 53$, which implies that chunk 2 can accommodate $c_2 = 21$ bits.
- The remaining bins (3-6) contribute to lowest order terms and hence they place no constraints on the splittings. In other words, $c_3 = 53$.

²While some of this can be addressed within the FP64 number, since it is a floating point number, there is the possibility of losing precision in the conversion.

³We will see that choosing k to be relative small naturally occurs in high-performance algorithms for GEMM. If k is smaller or larger, appropriate adjustments can be made.

The total number of bits stored with cascaded representataion is now actually $22 + 21 + 21 + 53 = 117$ which is more than the number of bits in the mantissa of a FP64x2 number (if there is no lucky gap). This means intermediate results are potentially accumulated in a precision higher than FP64x2 accommodates. Summation within bins can be in FP64 arithmetic. Summation across bins 0 through 2 must be performed in FP64x2 addition or with quick two-sum arithmetic [7]. Summation across bins 3 through 6 can be done in FP64 arithmetic, since $c_3 = 53$ implies that these terms are not even attempted to be done error-free. To further preserve accuracy, the adding of contributions across bins starts with bin 6 and ends with bin 0.

The computation in (3) can be reformulated as the computation of the sixteen terms

$$\begin{pmatrix} x_0^T \\ \sigma_1 x_1^T \\ \sigma_2 x_2^T \\ \sigma_3 x_3^T \end{pmatrix} \begin{pmatrix} y_0 & | & \sigma_1 y_1 & | & \sigma_2 y_2 & | & \sigma_3 y_3 \end{pmatrix} = \begin{pmatrix} x_0^T y_0 & | & \sigma_1 x_0^T y_1 & | & \sigma_2 x_0^T y_2 & | & \sigma_3 x_0^T y_3 \\ \sigma_1 x_1^T y_0 & | & \sigma_1^2 x_1^T y_1 & | & \sigma_1 \sigma_2 x_1^T y_2 & | & \sigma_1 \sigma_3 x_1^T y_3 \\ \sigma_2 x_2^T y_0 & | & \sigma_2 \sigma_1 x_2^T y_1 & | & \sigma_2^2 x_2^T y_2 & | & \sigma_2 \sigma_3 x_2^T y_3 \\ \sigma_3 x_3^T y_0 & | & \sigma_3 \sigma_1 x_3^T y_1 & | & \sigma_3 \sigma_2 x_3^T y_2 & | & \sigma_3^2 x_3^T y_3 \end{pmatrix}$$

followed by the addition of these terms, yielding a single scalar.

Finally, we observe an alternative for computing the sum of bins 3–6:

$$\begin{aligned} \text{bin 3-6} &= \sigma_3 x_0^T y_3 + \\ &\quad \sigma_1 \sigma_2 x_1^T y_2 + \sigma_1 \sigma_3 x_1^T y_3 + \\ &\quad \sigma_2 \sigma_1 x_2^T y_1 + \sigma_2^2 x_2^T y_2 + \sigma_2 \sigma_3 x_2^T y_3 + \\ &\quad \sigma_3 x_3^T y_0 + \sigma_3 \sigma_1 x_3^T y_1 + \sigma_3 \sigma_2 x_3^T y_2 + \sigma_3^2 x_3^T y_3 \\ &\quad \underbrace{\hspace{2cm}}_{\text{bin 3}} \quad \underbrace{\hspace{2cm}}_{\text{bin 4}} \quad \underbrace{\hspace{2cm}}_{\text{bin 5}} \quad \underbrace{\hspace{2cm}}_{\text{bin 6}} \\ &= \sigma_3 x_0^T y_3 + \sigma_1 x_1^T \underbrace{(\sigma_2 y_2 + \sigma_3 y_3)}_{\sigma_2 y_4} + \sigma_2 x_2^T \underbrace{(\sigma_1 y_1 + \sigma_2 y_2 + \sigma_3 y_3)}_{\sigma_1 y_5} \\ &\quad + \sigma_3 x_3^T \underbrace{(y_0 + \sigma_1 y_1 + \sigma_2 y_2 + \sigma_3 y_3)}_{y_6} \\ &= \sigma_3 x_0^T y_3 + \sigma_1 \sigma_2 x_1^T y_4 + \sigma_2 \sigma_1 x_2^T y_5 + \sigma_3 x_3^T y_6. \end{aligned}$$

This also shows how the approximate FP64x2 dot product can be cascaded into **ten** rather than sixteen FP64 dot products. Viewing chunks of x as rows of a $4 \times k$ matrix and chunks of y and related vectors as columns in a $k \times 7$ matrix, (3) can be formulated as

$$\begin{pmatrix} x_0^T \\ \sigma_1 x_1^T \\ \sigma_2 x_2^T \\ \sigma_3 x_3^T \end{pmatrix} \begin{pmatrix} y_0 & | & \sigma_1 y_1 & | & \sigma_2 y_2 & | & \sigma_3 y_3 & || & \sigma_2 y_4 & | & \sigma_1 y_5 & | & \tau_0 y_6 \end{pmatrix} = \begin{pmatrix} x_0^T y_0 & | & \sigma_1 x_0^T y_1 & | & \sigma_2 x_0^T y_2 & | & \sigma_3 x_0^T y_3 & || & * & | & * & | & * \\ \sigma_1 x_1^T y_0 & | & \sigma_1 \sigma_1 x_1^T y_1 & | & * & | & * & || & \sigma_1 \sigma_2 x_1^T y_4 & | & * & | & * \\ \sigma_2 x_2^T y_0 & | & * & | & * & | & * & || & * & | & \sigma_2 \sigma_1 x_2^T y_5 & | & * \\ * & | & * & | & * & | & * & || & * & | & * & | & \sigma_3 x_3^T y_6 \end{pmatrix}$$

followed by the summation of the elements or the appropriate contributions into bins and then the accumulation of those, in appropriate precision. Here the \star entries do not need to be computed.

We note that

$$\hat{x} = (x_0 + x_1 \sigma_1 + x_2 \sigma_2 + x_3 \sigma_3 + \hat{\Delta} x) \sigma, \text{ where } |\hat{\Delta} x| \leq \tilde{\epsilon}_{\text{mach}} \vec{j}.$$

In the symbol δx the δ touches the x to indicate this is one symbol to represent the error vector; $|\cdot|$ returns the element-wise absolute value; and \leq is an element-wise comparison; and \vec{j} is the vector of appropriate size of all ones. Letting χ_i equal the entry with maximal magnitude in x ,

$$\chi_i = \pm \cdot \beta_0 \beta_1 \cdots \times 2^t,$$

where $\beta_0 = 1$, the $\sigma = 2^{-t}$ in our discussion. Hence $|\chi_i| \leq 2^t \leq 2|\chi_i|$. We conclude that $\sigma \leq 2 \max_i |\chi_i|$ so that

$$|\delta x \sigma| \leq 2\tilde{\epsilon}_{\text{mach}} \max_i |\chi_i| \vec{j}.$$

Again, this is pessimistic given that the last chunk of the vector, x_3 carries a full FP64 remainder. In line with the reasoning that resulted in (2), this yields

$$\hat{x} = (x_0 + x_1\sigma_1 + x_2\sigma_2 + x_3\sigma_3)\sigma + \delta x \sigma,$$

where

$$|\delta x \sigma| \leq \min \left(2\tilde{\epsilon}_{\text{mach}} \max_i |\chi_i| \vec{j}, \epsilon_{\text{mach}} |x| \right). \quad (4)$$

Here $\epsilon_{\text{mach}} = 2^{-53}$ and $\tilde{\epsilon}_{\text{mach}} = 2^{-117}$ when $c_0 = 22$, $c_1 = c_2 = 21$, and $c_3 = 53$.

3.4 Cascading matrices and GEMM

We are now ready to discuss how to cascade FP64x2 matrices \hat{A} and \hat{B} and approximately compute $\hat{A}\hat{B}$. Here we restrict the “inner size” of the matrices to equal the k discussed in Section 3.3 since later we will see that high-performance implementations of GEMM block the operands in a way that imposes that restriction. Such a GEMM is often referred to as a *rank- k update*.

Now

$$\begin{aligned} \hat{A} &= \Sigma (A_0 + \sigma_1 A_1 + \sigma_2 A_2 + \sigma_3 A_3) \\ \hat{B} &= (B_0 + \sigma_1 B_1 + \sigma_2 B_2 + \sigma_3 B_3) T, \end{aligned}$$

where Σ and T are the diagonal matrices⁴ that appropriately scale the rows of \hat{A} (which become \hat{x} in the dot products discussed in Section 3.3) and columns of \hat{B} (which become \hat{y} in the dot products discussed in Section 3.3). The cascading of rows of \hat{A} and columns of \hat{B} follow exactly the discussion in the last section, since elements of the product are computed with dot products.

Then

$$\begin{aligned} \hat{A}\hat{B} \approx \Sigma & (A_0 B_0 + \sigma_1 A_0 B_1 + \sigma_2 A_0 B_2 + \sigma_3 A_0 B_3 \\ & + \sigma_1 A_1 B_0 + \sigma_1^2 A_1 B_1 + \sigma_1 \sigma_2 A_1 B_2 + \sigma_1 \sigma_3 A_1 B_3 + \\ & + \sigma_2 A_2 B_0 + \sigma_2 \sigma_1 A_2 B_1 + \sigma_2^2 A_2 B_2 + \sigma_2 \sigma_3 A_2 B_3 + \\ & + \sigma_3 A_3 B_0 + \sigma_3 \sigma_1 A_3 B_1 + \sigma_3 \sigma_2 A_3 B_2 + \sigma_3^2 A_3 B_3) T. \end{aligned} \quad (5)$$

The point is that one can approximately compute the FP64x2 GEMM in terms of 16 FP64 GEMMs, extending the observations about dot products. This means that

- D_0 , D_1 , and D_2 are picked as discussed in Section 3.3.
- Elements within rows of \hat{A} must be chunked conformally.
- Elements within columns of \hat{B} must be chunked conformally.

The terms in bins 0–2 are computed exactly. Unless “catastrophic cancellation” happens, the contributions of those bins will contribute the most significant bits of the results.

⁴Recall that multiplying a matrix from the left by a diagonal matrix scales its rows by the corresponding element of the diagonal matrix. Similarly, multiplying a matrix from the right by a diagonal matrix scales its columns.

Again, bins 3–6 can be combined, since they contribute to lower order terms.

$$\begin{aligned}
\text{bin 3-6} &= \sigma_3 A_0 B_3 + \\
&\quad \sigma_1 \sigma_2 A_1 B_2 + \sigma_1 \sigma_3 A_1 B_3 + \\
&\quad \sigma_2 \sigma_1 A_2 B_1 + \sigma_2^2 A_2 B_2 + \sigma_2 \sigma_3 A_2 B_3 + \\
&\quad \underbrace{\sigma_3 A_3 B_0}_{\text{bin 3}} + \underbrace{\sigma_3 \sigma_1 A_3 B_1}_{\text{bin 4}} + \underbrace{\sigma_3 \sigma_2 A_3 B_2}_{\text{bin 5}} + \underbrace{\sigma_3^2 A_3 B_3}_{\text{bin 6}} \\
&= A_0 B_3 \sigma_3 + A_1 \sigma_1 \underbrace{(B_2 \sigma_2 + B_3 \sigma_3)}_{B_4 \sigma_2} + A_2 \sigma_2 \underbrace{(B_1 \sigma_1 + B_2 \sigma_2 + B_3 \sigma_3)}_{B_5 \sigma_1} \\
&\quad + \sigma_3 A_3 \underbrace{(B_0 + \sigma_1 B_1 + \sigma_2 B_2 + \sigma_3 B_3)}_{B_6}. \\
&= \sigma_3 A_0 B_3 + \sigma_1 \sigma_2 A_1 B_4 + \sigma_2 \sigma_1 A_2 B_5 + \sigma_3 A_3 B_6
\end{aligned}$$

This also shows how the approximate FP64x2 GEMM can be cascaded into **ten** rather than sixteen FP64 multiplications. Now (5) can be depicted as the computation of

$$\begin{pmatrix} A_0 \\ \sigma_1 A_1 \\ \sigma_2 A_2 \\ \sigma_3 A_3 \end{pmatrix} \left(B_0 \mid \sigma_1 B_1 \mid \sigma_2 B_2 \mid \sigma_3 B_3 \parallel \sigma_2 B_4 \mid \sigma_1 B_5 \mid B_6 \right) = \begin{pmatrix} A_0 B_0 & \sigma_1 A_0 B_1 & \sigma_2 A_0 B_2 & \sigma_3 A_0 B_3 & \star & \star & \star \\ \sigma_1 A_1 B_0 & \sigma_1^2 A_1 B_1 & \star & \star & \sigma_1 \sigma_2 A_1 B_4 & \star & \star \\ \sigma_2 A_2 B_0 & \star & \star & \star & \star & \sigma_2 \sigma_1 A_2 B_5 & \star \\ \star & \star & \star & \star & \star & \star & \sigma_3 A_3 B_6 \end{pmatrix} \quad (6)$$

followed by the summation of the elements or the appropriate contributions into bins and then the accumulation of those, in appropriate precision. Here the \star entries do not need to be computed.

We finish by noting that from (4) it follows that

$$\widehat{A} = \Sigma(A_0 + \sigma_1 A_1 + \sigma_2 A_2 + \sigma_3 A_3) + \Sigma \Delta A,$$

where

$$|\Sigma \Delta A| \leq \min \left(2\tilde{\epsilon}_{\text{mach}} D_A J, \epsilon_{\text{mach}} |\widehat{A}| \right) \text{ with } D_A = \text{diag}(\max_j |\alpha_{0,j}|, \max_j |\alpha_{1,j}|, \dots).$$

Here, in ΔA the Δ touches the A to indicate this is one symbol to represent the error matrix; $|\cdot|$ returns the element-wise absolute value; and \leq is an element-wise comparison J is the matrix of appropriate size of all ones.

If $\delta \alpha_{i,j}$ denotes the error incurred when cascading element $\alpha_{i,j}$, this captures that

$$|\delta \alpha_{i,j}| \leq \min \left(2\tilde{\epsilon}_{\text{mach}} \max_j |\alpha_{i,j}|, \epsilon_{\text{mach}} |\alpha_{i,j}| \right).$$

An interpretation of this is that storing a real-valued matrix as a FP64x2 matrix incurs an element-wise relative error. Cascading a FP64x2 matrix \widehat{A} with our method incurs an error in a given element that is proportional to the magnitude of the largest element in the same row for \widehat{A} . However, because the last chunk of a given element captures the remainder of what it left when the other chunks are subtracted from the original FP64x2 number, when those other chunks equal zero, what is left is a FP64 approximation and hence the error is never worse than what is incurred when storing from FP64x2 to FP64.

3.5 Analysis

We here provide a preliminary forward error analysis of casting a FP64x2 GEMM as a cascaded multiplication in FP64. We only analyze how the error introduced by transforming the matrices propagates into error in the matrix multiplication under the conjecture that this is the primary source of significant error beyond the usual error introduced when computing with floating point arithmetic. We compare the result with standard error bounds for GEMM in a given precision, in this case FP64x2.

We start with a simple worst-case example of how cascading can reduce accuracy in a dot product, the building block of a matrix multiplication. Let

$$\hat{x} = \begin{pmatrix} 1 \\ \epsilon \end{pmatrix} \text{ and } \hat{y} = \begin{pmatrix} 0 \\ 1 \end{pmatrix}.$$

If $\epsilon < 2^{-64}$, then cascading \hat{x} and \hat{y} yields

$$\underbrace{\begin{pmatrix} 1 \\ \epsilon \end{pmatrix}}_{\hat{x}} \approx \underbrace{(1)}_{\sigma} \left(\underbrace{\begin{pmatrix} 1 \\ \epsilon \end{pmatrix}}_{x_0} + \sigma_1 \underbrace{\begin{pmatrix} 0 \\ 0 \end{pmatrix}}_{x_1} + \sigma_2 \underbrace{\begin{pmatrix} 0 \\ 0 \end{pmatrix}}_{x_2} + \sigma_3 \underbrace{\begin{pmatrix} 0 \\ \text{fl}_{\text{FP64}}(\epsilon/\sigma_3) \end{pmatrix}}_{x_3} \right),$$

where $\text{fl}_{\text{FP64}}(\zeta)$ equals the FP64 approximation to ζ , and

$$\underbrace{\begin{pmatrix} 0 \\ 1 \end{pmatrix}}_{\hat{y}} \approx \underbrace{(1)}_{\tau} \left(\underbrace{\begin{pmatrix} 0 \\ 1 \end{pmatrix}}_{y_0} + \sigma_1 \underbrace{\begin{pmatrix} 0 \\ 0 \end{pmatrix}}_{y_1} + \sigma_2 \underbrace{\begin{pmatrix} 0 \\ 0 \end{pmatrix}}_{y_2} + \sigma_3 \underbrace{\begin{pmatrix} 0 \\ 0 \end{pmatrix}}_{y_3} \right).$$

Then $\hat{x}^T \hat{y} = \epsilon$ when computed in FP64x2 arithmetic (incurring no error in this very special case) and $\tilde{x}^T \tilde{y} = \text{fl}_{\text{FL64}}(\epsilon)$ when computed as a cascaded dot product, incurring no error other than that incurred when cascading \hat{x} . In other words, the accuracy is no better than if the computation had been performed in FP64 arithmetic because the entire vector \hat{x} is conformally chunked.

Assuming \hat{A} is $m \times k$ and \hat{B} is $k \times n$,

$$\begin{aligned} \widehat{AB} &= [\underbrace{\Sigma(A_0 + \sigma_1 A_1 + \sigma_2 A_2 + \sigma_3 A_3)}_{\tilde{A}} + \Sigma \Delta A] [\underbrace{(B_0 + \sigma_1 B_1 + \sigma_2 B_2 + \sigma_3 B_3)T}_{\tilde{B}} + \Delta B T] \\ &= \tilde{A} \tilde{B} + E, \end{aligned}$$

where

$$E = \tilde{A} \Delta B T + \Sigma \Delta A \tilde{B} + \Sigma \Delta A \Delta B T$$

captures an error that ignores the error in computing bin 3-6 and in the accumulation of the bins, which we conjecture is minor by comparison. Now

$$\begin{aligned} |E| &= |\tilde{A} \Delta B T + \Sigma \Delta A \tilde{B} + \Sigma \Delta A \Delta B T| \\ &\leq |\tilde{A}| |\Delta B T| + |\Sigma \Delta A| |\tilde{B}| + |\Sigma \Delta A| |\Delta B T| \\ &\leq |\tilde{A}| \min(2\tilde{\epsilon}_{\text{mach}} J D_B, \epsilon_{\text{mach}} |\tilde{B}|) + \min(2\tilde{\epsilon}_{\text{mach}} D_A J, \epsilon_{\text{mach}} |\tilde{A}|) |\tilde{B}| \\ &\quad + \min(2\tilde{\epsilon}_{\text{mach}} D_A J, \epsilon_{\text{mach}} |\tilde{A}|) \min(2\tilde{\epsilon}_{\text{mach}} J D_B, \epsilon_{\text{mach}} |\tilde{B}|) \\ &= 2\tilde{\epsilon}_{\text{mach}} \left[|\tilde{A}| J D_B + D_A J |\tilde{B}| \right] + 4\tilde{\epsilon}_{\text{mach}}^2 k D_A J D_B. \end{aligned}$$

Since the ‘‘min’’s make the bound hard to analyze, we analyze two cases separately:

- Case 1:

$$\begin{aligned}
|E| &\leq |\tilde{A}| \min\left(2\tilde{\epsilon}_{\text{mach}}JD_B, \epsilon_{\text{mach}}|\tilde{B}|\right) + \min\left(2\tilde{\epsilon}_{\text{mach}}D_AJ, \epsilon_{\text{mach}}|\tilde{A}|\right) |\tilde{B}| \\
&\quad + \min\left(2\tilde{\epsilon}_{\text{mach}}D_AJ, \epsilon_{\text{mach}}|\tilde{A}|\right) \min\left(2\tilde{\epsilon}_{\text{mach}}JD_B, \epsilon_{\text{mach}}|\tilde{B}|\right) \\
&\leq |\tilde{A}|2\tilde{\epsilon}_{\text{mach}}JD_B + 2\tilde{\epsilon}_{\text{mach}}D_AJ|\tilde{B}| + 4\tilde{\epsilon}_{\text{mach}}^2D_AJJD_B \\
&= 2\tilde{\epsilon}_{\text{mach}}\left[|\tilde{A}|JD_B + D_AJ|\tilde{B}|\right] + 4k\tilde{\epsilon}_{\text{mach}}^2D_AJD_B,
\end{aligned}$$

since $JJ = kJ$ (where each J is of appropriate size). This gives us an element-wise bound. For reference, compare this to the established bound [15] for computing $\hat{A}\hat{B}$ in FP64x2 arithmetic of

$$\hat{A}\hat{B} = \text{fl}_{\text{FP64x2}}(\hat{A}\hat{B}) + F,$$

where $\text{fl}_{\text{FP64x2}}(\hat{A}\hat{B})$ equals the result of computing the multiplication in FP64x2 arithmetic, with

$$|F| \leq \frac{k\hat{\epsilon}_{\text{mach}}}{1 - k\hat{\epsilon}_{\text{mach}}} |\hat{A}|\hat{B}| \approx k\hat{\epsilon}_{\text{mach}}|\hat{A}|\hat{B}|$$

since k is assumed to be relatively small.

Noting that $\|J\|_F = \sqrt{pq}$ for a $p \times q$ matrix J , $\|D_A\|_F \leq \|A\|_F$, and $\|D_B\|_F \leq \|B\|_F$, gives us a bound in terms of the Frobenius norm of

$$\begin{aligned}
\|E\|_F &\leq 2\tilde{\epsilon}_{\text{mach}}\left[\sqrt{mk}\|\tilde{A}\|_F\|\tilde{B}\|_F + \sqrt{kn}\|\hat{A}\|_F\|\tilde{B}\|_F\right] + 4\tilde{\epsilon}_{\text{mach}}^2\sqrt{mnk}\|\tilde{A}\|_F\|\tilde{B}\|_F \\
&\approx \left(2\tilde{\epsilon}_{\text{mach}}(\sqrt{mk} + \sqrt{kn}) + 4\tilde{\epsilon}_{\text{mach}}^2\sqrt{mnk}\right)\|\hat{A}\|_F\|\tilde{B}\|_F \approx 2^{-116}(\sqrt{mk} + \sqrt{kn})\|\hat{A}\|_F\|\tilde{B}\|_F.
\end{aligned}$$

Contrast this with

$$\|F\|_F \leq \frac{k\hat{\epsilon}_{\text{mach}}}{1 - k\hat{\epsilon}_{\text{mach}}} \|\hat{A}\|_F\|\hat{B}\|_F \approx k2^{-106}\|\hat{A}\|_F\|\hat{B}\|_F.$$

- Case 2:

$$\begin{aligned}
|E| &\leq |\tilde{A}| \min\left(2\tilde{\epsilon}_{\text{mach}}JD_B, \epsilon_{\text{mach}}|\tilde{B}|\right) + \min\left(2\tilde{\epsilon}_{\text{mach}}D_AJ, \epsilon_{\text{mach}}|\tilde{A}|\right) |\tilde{B}| \\
&\quad + \min\left(2\tilde{\epsilon}_{\text{mach}}D_AJ, \epsilon_{\text{mach}}|\tilde{A}|\right) \min\left(2\tilde{\epsilon}_{\text{mach}}JD_B, \epsilon_{\text{mach}}|\tilde{B}|\right) \\
&\leq |\tilde{A}|\epsilon_{\text{mach}}|\tilde{B}| + \epsilon_{\text{mach}}|\tilde{A}|\|\tilde{B}\| + \epsilon_{\text{mach}}|\tilde{A}|\epsilon_{\text{mach}}|\tilde{B}| \\
&= 2\epsilon_{\text{mach}}|\tilde{A}|\|\tilde{B}\| + \epsilon_{\text{mach}}^2\tilde{A}|\tilde{B}| \approx 2\epsilon_{\text{mach}}|\tilde{A}|\|\tilde{B}\|,
\end{aligned}$$

from which we conclude that in the worst case, the element-wise error introduced by cascading the matrices is bounded by a value close to that incurred by computing with FP64 arithmetic.

We again stress that this analysis is only meant to give an idea of the kinds of errors that are introduced by approximating the matrices. In Section 6.4 we discuss what additional analysis remains to be performed.

3.6 Detecting cancellation error

Dot products, the implicit or explicit cornerstone of GEMM, can suffer severe cancellation errors which lead to less accurate results, especially for vectors near orthogonal. In most floating-point calculations this phenomenon is difficult to detect while it's happening unless one does very intrusive (and thus not performance or power friendly) checking before and after each FMA.

A cascaded dot product (within GEMM) combines fixed-point and floating-point calculation so that highest order bits of the result are always computed error-free in fixed-point. Because we always get exact results in bins 0, 1, and 2, the leading bits⁵ D_2 (≈ 64) bits are calculated error-free, followed by some FP64 calculations in bin 3–6 that get similar accuracy as one might expect from FP64. This might be far better than FP64x2 where the results from both parts suffer with standard FP64 (106-bit mantissa) errors. However, there is no guarantee that we calculate the first *most significant* 64 bits error-free,

⁵Notice that we can't say most significant here.

because there may be leading zero bits in the result. In the worse case scenario, bins 0-2 may be all zeroes, in which case the final accuracy will be closer to that of FP64 than FP64x2, as discussed before.

With the proposed approach, this phenomena can be relatively cheaply detected. Without going into details, by monitoring how many leading zeroes result in bins 0–3, cancellation can be flagged. We further comment on this in Section 4.4.

4 Practical considerations

We illustrate the viability of the scheme proposed in the last section by leveraging principles that underly the BLAS-like Library Instantiation Software (BLIS) framework [32, 33]. BLIS strives to enable optimizing performance while minimizing the amount of code that must be customized for a new architecture. Experience with many generations of CPUs has demonstrated that performance that rivals that of the best implementations can be achieved while keeping the effort manageable.

The proposed scheme for computing GEMM via cascaded matrices entails three phases:

Phase one: Splitting the matrices into its cascading components. The technical details of our approach to this can be found in Appendix A.

Phase two: Computing the various products within a bin exploiting a high-performing FP64 matrix multiplication.

Phase three: Adding across the bins in FP64x2 precision to obtain the final answer.

We now examine how to integrate these into a high-performance implementation.

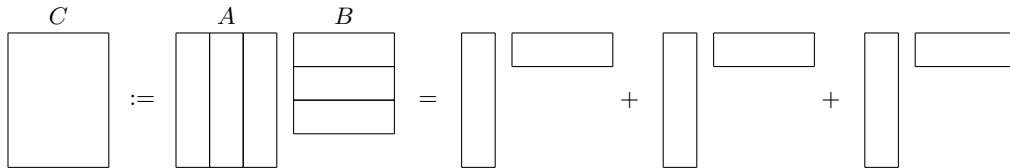
4.1 High-performance implementation of GEMM

Most current high-performance implementations of GEMM for CPUs, including BLIS, implement Goto’s Algorithm [12]. The BLIS instantiation of this algorithm exposes five loops (implemented in the C programming language) around a *micro-kernel* (implemented in assembly code or with intrinsic functions) as illustrated in Figure 3. The micro-kernel updates a $m_R \times n_R$ *micro-tile* of C , C_{ij} , by multiplying a $m_R \times k_C$ *micro-panel* of A times a $k_C \times n_R$ micro-panel of B . On a typical architecture, the micro-tile of C is kept in registers while the micro-panel of B is streamed from the L1 cache and the micro-panel of A is streamed from the L2 cache. In order to access memory with stride one (consecutive access), blocks of A and row panels of B are packed (rearranged) at strategic points in the algorithm [14]. Generally, blocking parameters can be determined analytically [21]. One advantage of exposing the five loops around the micro-kernel in C is that it presents multiple loops where thread-level parallelism can be introduced [27, 32].

The original GotoBLAS implementation required the computation related to the two loops around the micro-kernel and the micro-kernel to be customized in assembly code for a given architecture. BLIS reduces this to just the micro-kernel.

4.2 Simple: FP64x2 GEMM via ten FP64 GEMMs

An important consequence of Goto’s algorithm is that it achieves its high performance already for rank-k updates with $k = k_C$ ($= 256$ on our target architecture discussed in Section 5.1). This allows us to stage GEMM as a sequence of rank-k updates:



This fits with the discussion in Sections 3.4, where k had to be constrained to be relatively small. This has the added advantage that it limits the workspace required for the cascaded matrices.

A simple approach to implement FP64x2 GEMM via ten FP64 GEMMs is now to explicitly cascade a column panel of FP64x2 matrix \hat{A} into four FP64 matrices, requiring $4 \times m \times k_C$ FP64 workspace, and

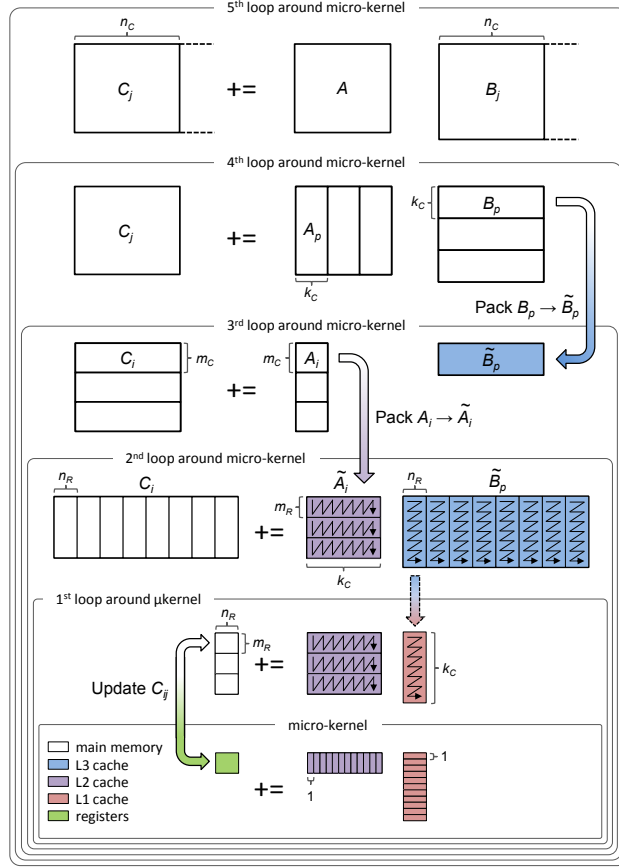


Figure 3: The BLIS refactoring of the GotoBLAS algorithm for GEMM as five loops around the microkernel. This diagram, which is often used when explaining the fundamental techniques that underly the BLIS implementation of GEMM, was modified from a similar image first published in [31] and is used with permission.

a row panel of \hat{B} into seven FP64 matrices, requiring $7 \times kc \times n$ FP64 workspace. The ten FP64 GEMMs in (6) can be computed by making calls to a high-performing DGEMM (FP64 GEMM) implementation like the one provided by BLIS, accumulating these into the four bins 0, 1, 2, and 3-6 each of size $m \times n$ FP64 numbers. Finally (or after each individual bin is computed), the results of these computations are added into C , via FP64x2 additions, adding in first bin 3-6, then bin 2, bin 1, and lastly bin 0, so that terms that are likely lower precision are accumulated in first. After this, Σ and T are applied, scaling the rows and columns of the result.

The problem with this naive implementation is that it requires considerable additional workspace to accommodate the splits of matrix A and B as well as the bins of matrix C . A careful ordering of the computation can reduce the required space for accumulating the bins. Performance is negatively impacted in this naive approach by the requirement that data be moved between memory layers repetitively as matrices B and A are cascaded and C is assembled from the bins.

4.3 BLIS-like: FP64x2 GEMM via ten FP64 GEMMs

The kind of overhead incurred by a naive cascaded multiplication is akin to the kind of overhead that makes a naive implementation of Strassen's algorithm [28] impractical except for very large problem sizes. In [17] it was shown how integrating Strassen's algorithm into an appropriate level of the BLIS GEMM

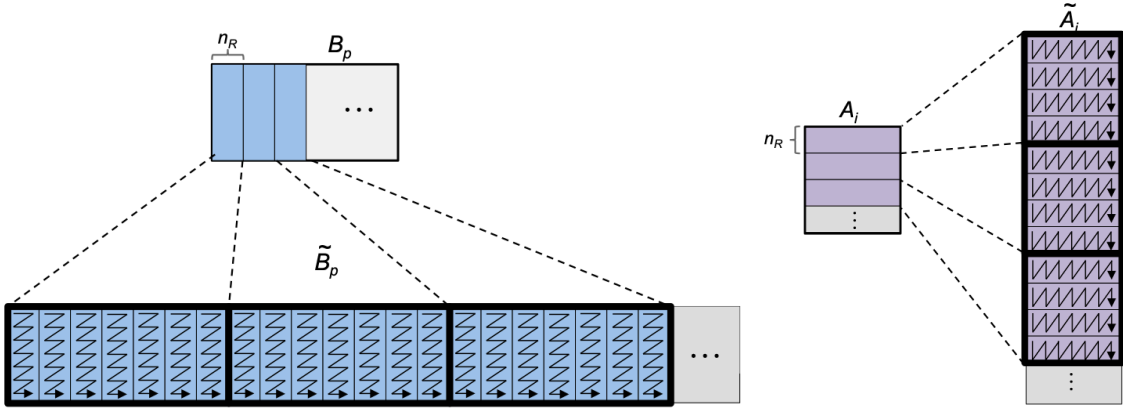


Figure 4: Left: Packing layout for a panel of B . Right: Packing layout for a block of A .

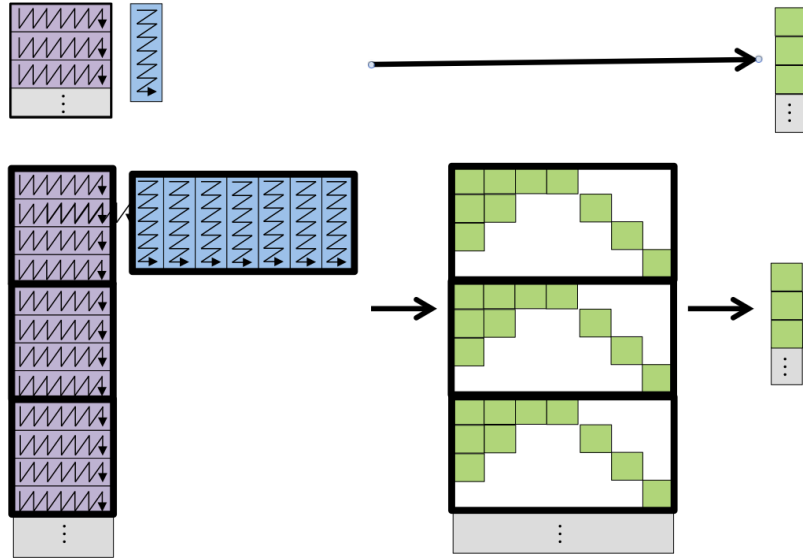


Figure 5: Top: Operation Goto's Algorithm performs in first loop around the micro-kernel. Bottom: Operation performed with cascaded matrices by first loop around the micro-kernel.

algorithm in Figure 3 it was possible to reduce that overhead so that high performance is achieved even for smaller matrices. Similar techniques can be employed for the cascaded matrix-multiplication as we now describe.

This approach requires a number of changes to the BLIS framework for GEMM:

- During the packing of a row panel of B , FP64x2 micro-panels need to be cascaded into the seven FP64 micro-panels, as illustrated in Figure 4. This suggests that the blocksize n_C be divided by seven so that the packed row panel of B has the same footprint in the L3 cache⁶.
- During the packing of a block of A , FP64x2 micro-panels need to be cascaded into the four FP64 micro-panels, as illustrated in Figure 4. This suggests dividing the blocksize m_C by four so that the packed block of a has the same footprint in the L2 cache.

⁶In practice, n_C is typically considerably smaller than the L3 cache can accommodate, and hence in practice we divide this by four.

- The “packed block of A times cascaded micro-panel of B ” now for each original micro-panel of A requires ten calls to the micro-kernel that compute then micro-tiles. As part of the execution of the micro-kernel, these contributions can be accumulated into the four bins. These additional calls to the micro-kernel are made by increasing the iterations of the first loop around the micro-kernel by four, and the second loop around the micro-kernel by seven. As indicated by (6) all possible products need not be computed.
- The final results is accumulated into the appropriate micro-tile of C , as illustrated in Figure 5, and scaled by applying Σ and T . This is done after the first loop around the micro-kernel to ensure the various bins remain in the L2 cache during this computation.

Importantly, all the described changes lie within the C code that implements GEMM. Micro-kernels that are already part of BLIS can be reused as-is. These changes do not effect the threading infrastructure already present in BLIS, enabling multi-threading for this implementation.

4.4 Adding detection of cancellation errors

Detection of cancellation, as hinted at in Section 3.6, can be incorporated into the algorithm in the step where a $m_C \times n_R$ micro-panel of \hat{C} is assembled from the various bins. This allows cancellation to be detected for multiplications where $k \leq k_C$. The current implementation does not attempt to perform any correction if such cancellation is found.

5 Experimental evaluation

We provide results in support of the proposed approach by reporting performance and accuracy results.

5.1 Performance experiments

We first report preliminary results of the FP64x2 GEMM via ten FP64 GEMMs implementation. As discussed, the simple implementation proposed in Subsection 4.2 can only become high performing for very large matrices and hence we only give performance results for the BLIS-like implementation.

As is customary for reporting performance of GEMM-like operations, we report the rate of computation in billions of FP64 (double precision) floating point operations per second (FLOPS). For comparison, the rate at which the BLIS implementation of DGEMM computes is given, using a $2mnk$ count for multiplying a $m \times k$ matrix times a $k \times n$ matrix. For the FP64x2 cascaded multiply, an operation count of $10 \times 2mnk4$ is used. In the experiments, all matrices are square.

The performance experiments were conducted on an Intel Core i7-7700K CPU with 4 cores. Each core executes at 4.20 GHz with a max turbo frequency of 4.50 GHz, providing a single-core peak performance of 72 GFLOPS in double precision. The 8 MB L3 cache is shared between all four cores, while each core has a private 256 KB L2 and 32 KB L1 cache. The installed OS is Ubuntu 18.04 running the Linux 4.15.0 kernel. BLIS version 0.8.1 was used in these experiments for the DGEMM performance curves.

Performance results are given in Figure 6. In the experiments, the cancellation detection mechanism is activated, but no correction is performed if a possible cancellation situation is detected. In the figure on the left, we report performance as a function of size, for square matrices. Here, the top of the graph represents peak performance. The same data is presented in the figure on the right, except that the slowdown relative to DGEMM is given. Since ten FP64 GEMMs are performed, one would expect to at best observe only a $10\times$ slowdown. This ideal is not achieved due to the overhead incurred by cascading matrices and summing results.

Our primary result is that our final algorithm seems to be similar to DGEMM efficiency. That is, we incur a slight overhead due to the cascading of the matrices into its chunks (phase one), and the gluing together of matrices in the end (phase three), but it’s only slight. The final algorithm does 10 DGEMM calls, and it has $10\times$ the flop count, but tends to run $10\text{-}13\times$ slower than DGEMM.

We do not report performance for a FP64x2 implementation. The primary reasons are that, since FP64x2 arithmetic would be emulated in software rather than hardware, the numbers would simply not be competitive. Moreover, any implementation would be subject to questions of whether it was the highest performing that can be implemented, regardless of the attained performance.

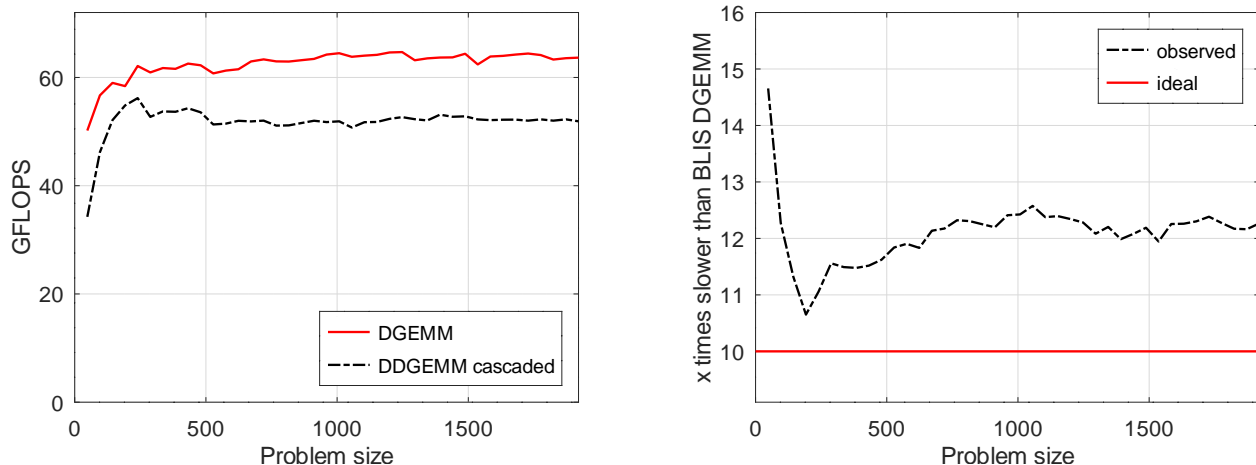


Figure 6: Comparing the sequential performance of BLIS DGEMM with FP64x2 cascaded matrix implementation. Left: GFLOPS attained for both BLIS DGEMM and FP64x2 cascaded matrices at various problem sizes ($m = n = k$). Right: Ratio of the execution time of FP64x2 cascaded matrix GEMM vs BLIS DGEMM (FP64 GEMM). Ideally, 10x slowdown is expected. Performance was obtained on an Intel Core i7-7700K CPU.

5.2 Accuracy experiments

A question is how accuracy is affected by casting FP64x2 GEMM in terms of ten FP64 GEMMs. In this paper, we only address this empirically, by investigating two types of problems: GEMM with matrices filled with uniformly distributed random data in a given range (or, sometimes widely varying ranges) and matrices constructed so that GEMM is ill-conditioned. The experiments examine how the error experienced by our scheme compares to the error encountered by a true FP64x2 multiplication. We use FP128x2 (double-quad) for reference accuracy.

Uniformly random data experiments

For our experiments, we ran a series of tests over problems with points initially (pseudo-random uniform generator) picked in the given range. Uniformly random data doesn't tend to spot all irregularities associated with range, which is why we also added ill-conditioned and wide-ranging experiments. Unless otherwise stated, we ran the uniformly random experiments on $[-1, 1]$. We first picked a random FP64 number in the given range, and then added random bits in the mantissa past 53, up to 113, and used this as a FP128 number in the prescribed range. We then converted this FP128 number into non-overlapping double-double FP64x2 format. This typically means that even though our exponents are non-overlapping between the high and low part, that they don't have too wide of a gap (only up to 8 or so bits in the initial exponent.) However, this seemed good enough, since larger gaps would probably get lost in the noise of the experiment.

Wide-range data experiments

For this set of experiments, instead of picking numbers in a range randomly, we picked the exponent ranges themselves randomly, and then picked uniformly random mantissas within those ranges. Using this method, it is possible to have some dot products cover ranges like $[2^{-30}, 2^0]$, $[-2^{10}, 2^3]$, or any combination. For each row of matrix A and each column of matrix B , we first randomly picked exponents between 10^{-60} to 10^{20} , and next randomly assign a sign. This gives us a range $[x, y]$, from which we pick uniformly random numbers to fill in the the rows of matrix A and columns of B . This results in having as many possible different dot products, with different ranges on the inputs, as possible.

Ill-conditioned experiments

One would expect error to be worst when cancellation is encountered. For this reason, since matrix multiplication in effect computes an entry of $C = AB$ by taking the dot product of a row of A with a column of B , it pays to examine when a dot product of two non-zero vectors, x and y , with reasonable length yields a relatively small result compared to their initial norms. Recall that this happens when, for example, $\|x\|_2 \approx \|y\|_2 = 1$ and $x^T y$ is small. The smaller $x^T y$, the more subject to cancellation error the computation likely is.

An attempt to create matrices so that multiplication with them is ill-conditioned was proposed when testing XBLAS [34]. They wrote an excellent generator for generating two vectors whose dot product manages to hit major cancellation error, and therefore, to generate matrices for matrix multiplication, one could stuff generated vectors x into rows of A and generated vectors y into columns of B . While effective, this approach leads to problems just on the diagonal of the result matrix, and meaningless (potentially very well-conditioned) data elsewhere. It seems unfortunate to generate n^2 data but only have n elements of it be useful for testing purposes. We propose an approach that yields many more potentially ill-conditioned cases within each GEMM, thus leveraging the work to compute GEMM towards many more cases of interest.

We create matrices that incorporate a large number of dot products that induce cancellation. For now, assume that the matrices are all square ($m = n = k$). We start by generating (in high precision) matrix A to have mutually orthonormal rows, by generating a random matrix, computing its FP128 QR factorization (using quad Householder transformations), and setting A equal to the resulting Q . Next, we generate a matrix C by first choosing its elements to be small, with magnitude in the range $(t, 10t)$, where $t > 0$ is some small positive tolerance. We randomly pick these values to be positive or negative (that is, each final element of A is either in $(t, 10t)$ or $(-10t, -t)$.) We also randomly pick precisely one location in every column of C to equal 1. Next, we set $B = Q^T C$ in quad-arithmetic. What we notice is that

- In exact arithmetic $C = AB$, so with the exception of only one element per column, most of C will in exact arithmetic have values of magnitude t .
- The columns of C have length approximately equal to one (assuming $t > 0$ is small) and hence so do the columns of B , since multiplication by a unitary matrix, Q^T , preserves length.
- The computation of AB inherently involves many dot products that have the desired property of triggering cancellation.

The above description works with square matrices and may be modified for non-square matrices. Since the accuracy of finding the worst component-wise error is independent of the matrix dimensions, we only examined results from multiplying square ill-conditioned tests. Of interest now is how elements in the result matrix lose accuracy as measured by the component-wise relative error.

In our experiments, we focus on three choices for tolerance t :

- $t = 10^{-9}$, which can wipe out all accuracy when computing in single precision (FP32).
- $t = 10^{-14}$, which can wipe out all accuracy when computing in double precision (FP64).
- $t = 10^{-19}$, which can lead to significant loss of accuracy when computing in FP64x2 arithmetic, but will leave some accuracy.

For each of these choices, we ran experiments for a range of problem sizes, reporting in Figure 7 the average worst case component-wise errors over many runs with different generated matrices. The error is computed as the difference with the corresponding value in the result matrix when computed in very high (FP128x2) arithmetic. We note that by this measure, the accuracy of the cascaded multiply in these experiments is vastly superior to that of FP64x2.

In Figure 7 (Left), we report the maximal elementwise relative error when computing GEMM with a simple triple-nested loop in FP64x2 arithmetic and with our cascaded multiplication, for different choices of tolerance t . The same data is reported in Figure 7 (Right), which reports the ratio between the maximal element-wise relative errors encountered of the FP64x2 implementation and the cascaded multiplication. What we see is that our approach tends to be *more accurate* for the ill-conditioned experiments. We attribute this to the fact that the highest order bits are computed error-free regardless of the condition number. It is an encouraging result that wide-ranging data seems to behave as well

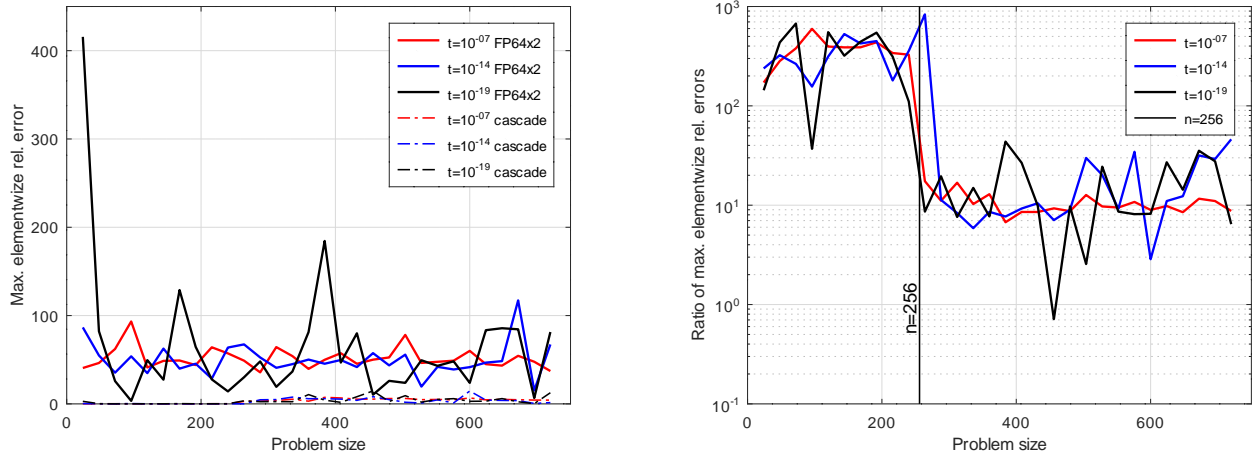


Figure 7: Error encountered for problems constructed to be ill-conditioned. Left: Maximum component-wise error for various choices of tolerance, for computation with FP64x2 arithmetic and with cascaded matrices. Right: Same data, presented as the ratio of error when computing with FP64x2 arithmetic and with cascaded multiplication.

as the well-conditioned data: it means that our methods handle range issues well, in contrast to most algorithms that employ fixed-point.

The drop in the ratio of size 256 can be expected: this is where, in the fourth loop around the micro-kernel, BLIS starts performing multiple rank-k updates. This means that each element in the result matrix is updated multiple times, incurring multiple conversions to FP64x2 storage. The point is that once we rounded down to FP64x2 accuracy, the benefits of storing intermediate results in higher precision diminishes.

A question is how accuracy is affected on an element-by-element basis. To answer this, we examine the relative error in all entries of matrix that results when multiplying two 240×240 matrices. In Figure 8 we report the ratio between the error encountered by the FP64x2 implementation and the cascaded matrix multiplication for different cases:

- Uniformly random data in $[-1, 1]$.
- Wide ranging data.
- Very badly conditioned: $t = 10^{-19}$.

Except for a very small number of elements, the cascaded multiplication yields the same or better accuracy.

In Figure 9, we again present the relative error in all elements of the result matrix, but this time sort the results by the error occurred by the cascaded multiplication. In other words, for a given element (value along the x-axis), the error incurred by the cascaded multiplication is reported in red and the error incurred by the FP64x2 implementation is reported in black. This shows how for well-conditioned problem the cascaded matrix multiplication is essentially uniformly better while for the ill-conditioned and wide-ranging inputs only in a few cases the FP64x2 implementation is better.

6 Conclusion and future opportunities

We reiterate that our focus on casting FP64x2 in terms of FP64 is merely a concrete illustration of a general principle. We choose to target bootstrapping FP64x2 accuracy from a high-performance FP64 implementation because BLIS as of the writing of this paper only supports double (FP64) and single

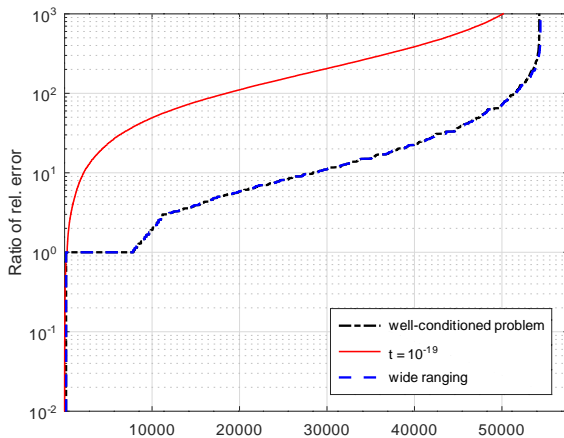


Figure 8: For this graph, the ratios (Cascaded divided by FP64x2) of relative accuracies of all elements of matrix $C = AB$ are reported, where all matrices involved are 240×240 . The elements are sorted by the value of the ratio, independently for each curve. Values (towards the left of the graph) that are less than 10^0 mean that FP64x2 is more accurate. The well-conditioned and wide ranging values experiments are virtually indistinguishable in the graph.

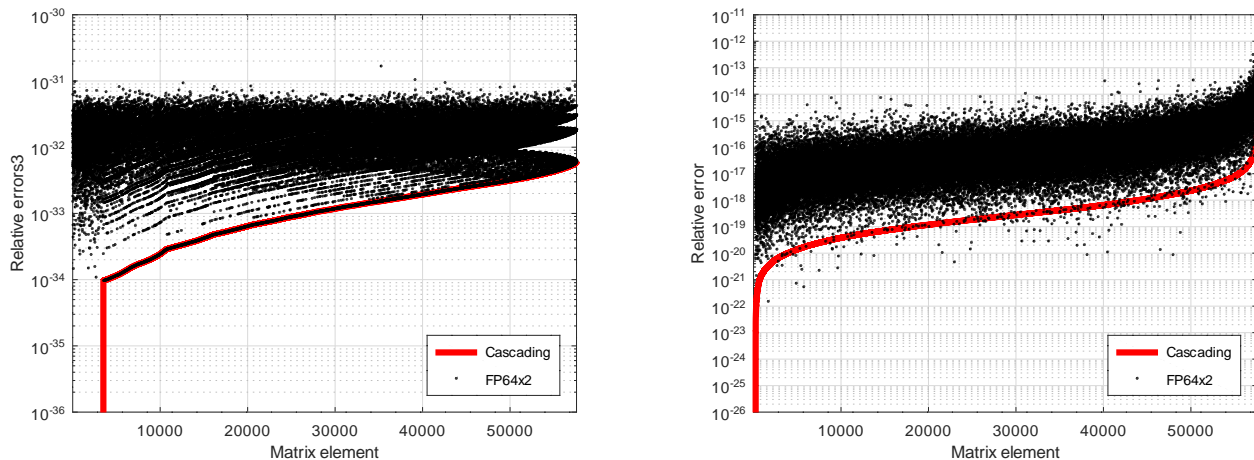


Figure 9: The relative error of all elements of matrix $C = AB$ are reported, where all matrices involved are 240×240 . The elements are sorted by the relative error incurred by the cascading matrix multiplication. The corresponding error incurred by FP64x2 is also reported. Left: well-conditioned experiments. Right: experiments with conditioning in the 10^{19} range. Be aware of the different scale reported along the y-axis.

(FP32) precision. By leveraging BLIS, we have demonstrated that high performance and accuracy can be achieved.

We now discuss a few extensions of the presented ideas that can be pursued in the future. We believe that these constitute several theses worth of work and can hence not be expected to be addressed in this initial study.

6.1 Safely dropping lower order bins

Consider Equation (3). Notice that *if* bin 0 has few or no leading zeroes, *then* any contributions from bins 4–6 may not affect the final stored result. This observation illustrates that under some conditions not all terms encountered in Equation (3) or Equation (5) may need to be computed. This observation generalizes to the case where computing a higher precision in terms of a lower precision requires t chunks. Roughly, if the highest order bin has few leading zero bits, only $t(t+1)/2$ terms may need to be computed. If the highest order bin has many zeroes (or is entirely zero), then additional terms may be required. The details are left to future research.

6.2 General casting of high precision in terms of low precision

We briefly discuss other cases where the general principle of cascading of matrices and multiplication can be of value.

6.2.1 FP32 in terms of bfloat16

Of particular interest these days is how to exploit various “half-precision” arithmetic (like bfloat16) that is starting to be supported in hardware [5]. Often, such bfloat16 arithmetic is 8-32 times faster than single precision (FP32) arithmetic⁷.

The proposed technique can be modified to accommodate cascading FP32 GEMM in terms of bfloat16 GEMM. In this case, FP32 numbers can be cascaded in terms of three bfloat16 chunks, with appropriately chosen D_0 , D_1 , and D_2 (as a function of k), and the cascaded multiplication can be cast in as few as 6 bfloat16 GEMMs [13]. The FP32 bit accumulation has a number of benefits: the bins do not first need to be accumulated separately, which simplifies the implementation, reduces the amount of workspace needed and changes how registers and caches are leveraged.

6.2.2 FP64 in terms of FP32

This case does not fit the cascading GEMM methodology well. The primary problem is that FP64 is supported in hardware on most current architectures. A secondary problem is that the number of chunks becomes unmanageable (we would need approximately 7 to 8 FP32 chunks with $k = 256$) and hence the number of FP32 GEMMs becomes impractical to gain any speedup.

6.2.3 FP64x3 in terms of FP64

Just as this paper shows how to use a cascading GEMM to approximate FP64x2 accuracy, one can approximate FP64x3 GEMM, by cascading the FP64x3 matrix into 6 FP64 chunks.

6.2.4 FP64 in terms of INT8

Modern architectures often support INT8 arithmetic with 32-bit accumulation. This lends itself to the cascading GEMM methodology, since to cascade the matrix into its chunks, the matrix is converted into fixed point numbers which can be stored in integers.

To compute FP64 GEMM by cascading it into INT8 chunks, we need at least seven 8-bit chunks to hold all the mantissa bits of an FP64 number (dropped bits can still occur in this method.) With seven chunks, we need at least 21 multiplies to obtain the result. The 32-bit accumulation provides the same benefits of as mentioned in section 6.2.1.

6.2.5 FP64x2 in terms of INT8

To support this scenario FP64x2 GEMM by cascading it into INT8 chunks, we need approximately 14 to 15 INT8 chunks and about 105 to 120 INT8 multiplies to obtain the result. On specific processors, INT8 may run faster than DGEMM. According to Figure 6, we can obtain an FP64x2 GEMM result in approximately 12x more time than DGEMM. Therefore, on any processor, where the peak INT8 operations runs at least $120/12 = 10$ times faster than double precision floating point operations, we

⁷Many times these operations can be memory-bound, and we don’t see the full theoretical speed-up

should see a net speedup using 15 cascading INT8 chunks using the methodology developed here. In fact, on many processors, INT8 GEMM may run 30x faster than DGEMM, making an INT8 version of cascading matrices potentially three times faster than the results we have presented.

The reason we do not present FP64x2 GEMM by cascading it into INT8 in this work is that we wanted to leverage existing kernels in BLIS, which meant basing an algorithm on DGEMM or SGEMM kernels. But the cascading matrices, in general, covers a wide range of problems not yet considered and further justifies the usefulness of this contribution.

6.2.6 Mixed precision

As of this writing, BLIS supports mixing domains and precision of the four data types (\mathbf{s} , \mathbf{d} , \mathbf{c} , \mathbf{z}) supported by the traditional BLAS [30] and is being extended to support new precisions (e.g. FP16 and FP64x2). Consider $C := AB + C$. Each of $\{A, B, C\}$ may have a different precision and/or the computation may be performed in a different precision than some or all of the operands. The current approach in BLIS is to convert all operands to the highest precision that is involved. The presented techniques can be leverage to, for example, selectively cascade operands to attain a desired precision while not being limited to the performance of the highest precision computations.

6.3 Targeting GPUs

As mentioned in Section 4.3, the techniques employed by the CPU implementation of cascading GEMM are similar to those used to implement a high-performance Strassen’s algorithm. In [18], it was shown how there is a parallel between the BLIS implementation of GEMM on CPUs and the CUTLASS implementation of GEMM on Nvidia GPUs [6]. This suggests that the approach may translate naturally to such GPUs.

6.4 Numerical analysis

In Section 3.5, we analyzed the impact of cascading matrices on the accuracy of a matrix multiplication. We discussed the issue and give theoretical insight, but did not solve all issues. While we have outlined a way to detect when we are suffering from severe cancellation error at almost no cost, the question that still remains is whether there is a way to know for sure that a result is more or less accurate than FP64x2. However, the fact that we have insight into cancellation error is already more than can be said about most other GEMM implementations.

6.5 Scaling/balancing methods

Mathematically, $\widehat{A}\widehat{B} = \widehat{A}F F^{-1}\widehat{B}$, where F is nonsingular. If F is diagonal, then this means that columns of \widehat{A} are scaled by the corresponding diagonal element of F and rows of \widehat{B} by the inverse of the corresponding diagonal element of F . Now, if a diagonal element of F is chosen to be small enough, the contribution of the corresponding column of \widehat{A} in a cascaded matrix multiplication can be reduced to FP64 accuracy, since the entries can become small relative to other entries in the same row of \widehat{A} . A similar argument can be made for scaling a row of \widehat{B} . In other words, how columns of \widehat{A} and/or rows of \widehat{B} are scaled matters.

This brings up the question whether a diagonal matrix F can be chosen to improve the accuracy of the cascaded matrix multiplication. We leave answering this to future research.

6.6 Analytical model of performance

An open question remains how to create an analytical model that estimates the performance of the proposed cascading GEMM techniques. Such a model would guide the choices of when, in the high performance GEMM algorithm, Phase 1 and Phase 3 can be performed to maximize the data reuse.

6.7 Supporting other level-3 BLAS-like functionality

All Level-3 BLAS algorithms can be written in terms of GEMM [19]. One naive solution then is to take a fast cascading GEMM implementation and re-use it as much as possible during any BLAS-3 routine. But also note that Phase 1 involves a lot of conversion, so integrating Phase 1 into specific calls of say TRSM can make the routine run even faster yet.

Acknowledgements

We thank members of the Science of High-Performance Computing (SHPC) group for their encouragement and feedback. This research was sponsored in part by the National Science Foundation (Award CSSI-2003921).

Any opinions, findings and conclusions or recommendations expressed in this material are those of the author(s) and do not necessarily reflect the views of the National Science Foundation (NSF).

References

- [1] David H. Bailey. A Fortran-90 double-double precision library. <http://crd.libl.gov/~dhbailey/mpdist>.
- [2] David H. Bailey. Extra high speed matrix multiplication on the Cray-2. *SIAM Journal of Scientific and Statistical Computing*, 8(3):603–607, 1988.
- [3] David H. Bailey. A Fortran-90 based multiprecision system. *ACM Trans Math Software*, 21:379–387, 1995.
- [4] Paolo Bientinesi and Robert A. van de Geijn. Goal-oriented and modular stability analysis. *SIAM J. Matrix Anal. Appl.*, 32(1):286–308, March 2011.
- [5] Intel Corporation. BFLOAT16—hardware numerics definition. White paper 338302-001US, Nov. 2018.
- [6] CUTLASS. CUTLASS: Cuda templates for linear algebra subroutines (v0.1.0). <https://github.com/NVIDIA/cutlass>, 2018.
- [7] T. J. Dekker. A floating-point technique for extending the available precision. *Numer. Math.*, 18(3):224–242, June 1971.
- [8] James Demmel and Yozo Hida. Accurate and efficient floating point summation. *SIAM Journal on Scientific Computing*, 25(4):1214–1248, 2004.
- [9] James Demmel, Yozo Hida, E. Jason Riedy, and Xiaoye S. Li. Extra-precise iterative refinement for overdetermined least squares problems. *ACM Trans. Math. Softw.*, 35(4), Feb. 2009.
- [10] Jack J. Dongarra, Jeremy Du Croz, Sven Hammarling, and Iain Duff. A set of level 3 basic linear algebra subprograms. *ACM Trans. Math. Softw.*, 16(1):1–17, March 1990.
- [11] Massimiliano Fasi, Nicholas J. Higham, Florent Lopez, Theo Mary, and Mantas Mikaitis. Matrix multiplication in multiword arithmetic: Error analysis and application to GPU tensor cores. *SIAM Journal on Scientific Computing*, 45(1):C1–C19, 2023.
- [12] Kazushige Goto and Robert A. van de Geijn. Anatomy of high-performance matrix multiplication. *ACM Trans. Math. Softw.*, 34(3: Article 12, 25 pages), May 2008.
- [13] Greg Henry, Ping Tak Peter Tang, and Alexander Heinecke. Leveraging the bfloat16 artificial intelligence datatype for higher-precision computations. In *2019 IEEE 26th Symposium on Computer Arithmetic (ARITH)*, pages 69–76, 2019.
- [14] Greg M. Henry. BLAS based on block data structures. Theory Center Technical Report CTC92TR89, Cornell University, Feb. 1992.
- [15] Nicholas J. Higham. *Accuracy and Stability of Numerical Algorithms*. Society for Industrial and Applied Mathematics, Philadelphia, PA, USA, second edition, 2002.

- [16] Jianyu Huang, Leslie Rice, Devin A. Matthews, and Robert A. van de Geijn. Generating families of practical fast matrix multiplication algorithms. In *2017 IEEE International Parallel and Distributed Processing Symposium (IPDPS)*, pages 656–667, May 2017.
- [17] Jianyu Huang, Tyler M. Smith, Greg M. Henry, and Robert A. van de Geijn. Strassen’s algorithm reloaded. In *Proceedings of the International Conference for High Performance Computing, Networking, Storage and Analysis, SC ’16*, pages 59:1–59:12, Piscataway, NJ, USA, 2016. IEEE Press.
- [18] Jianyu Huang, Chenhan D. Yu, and Robert A. van de Geijn. Strassen’s algorithm reloaded on gpus. *ACM Trans. Math. Softw.*, 46(1), March 2020.
- [19] Bo Kågström, Per Ling, and Charles van Loan. GEMM-based level 3 BLAS: High-performance model, implementations and performance evaluation benchmark. LAPACK Working Note #107 CS-95-315, Univ. of Tennessee, Nov. 1995.
- [20] Xiaoye S. Li, James Demmel, David H. Bailey, Greg Henry, Yozo Hida, Jimmy Iskandar, William Kahan, Suh Y. Kang, Anil Kapur, Michael C. Martin, Brandon J. Thompson, Teresa Tung, and Daniel J. Yoo. Design, implementation and testing of extended and mixed precision blas. *ACM Trans. Math. Softw.*, 28(2):152–205, June 2002.
- [21] Tze Meng Low, Francisco D. Igual, Tyler M. Smith, and Enrique S. Quintana-Ortí. Analytical modeling is enough for high-performance BLIS. *ACM Transactions on Mathematical Software*, 43(2):12:1–12:18, August 2016.
- [22] Devin A. Matthews. High-performance tensor contraction without transposition. *SIAM J. Sci. Comput.*, 40(1):C1–C24, January 2018.
- [23] Daichi Mukunoki, Katsuhisa Ozaki, Takeshi Ogita, and Toshiyuki Imamura. DGEMM using tensor cores, and its accurate and reproducible versions. In *High Performance Computing: 35th International Conference, ISC High Performance*, pages 230–248, June 2020.
- [24] Takeshi Ogita, Siegfried M. Rump, and Shin’ichi Oishi. Accurate sum and dot product. *SIAM J. Sci. Comput.*, 26(6):1955–1988, January 2005.
- [25] Katsuhisa Ozaki, Takeshi Ogita, Shin’ichi Oishi, and Siegfried M. Rump. Error-free transformations of matrix multiplication by using fast routines of matrix multiplication and its applications. *Numer. Algorithms*, 59(1):95–118, January 2012.
- [26] Siegfried M. Rump. Ultimately fast accurate summation. *SIAM J. Sci. Comput.*, 31(5):3466–3502, September 2009.
- [27] Tyler M Smith, Robert van de Geijn, Mikhail Smelyanskiy, Jeff R Hammond, and Field G Van Zee. Anatomy of high-performance many-threaded matrix multiplication. In *Parallel and Distributed Processing Symposium, 2014 IEEE 28th International*, pages 1049–1059. IEEE, 2014.
- [28] Volker Strassen. Gaussian elimination is not optimal. *Numer. Math.*, 13(4):354–356, August 1969.
- [29] Field G. Van Zee. Implementing high-performance complex matrix multiplication via the 1M method. *SIAM Journal on Scientific Computing*, 42(5):C221–C244, September 2020.
- [30] Field G. Van Zee, Devangi N. Parikh, and Robert A. van de Geijn. Supporting mixed-domain mixed-precision matrix multiplication within the blis framework. *ACM Transactions on Mathematical Software*, 47(2):12:1–12:26, April 2021.
- [31] Field G. Van Zee and Tyler M. Smith. Implementing high-performance complex matrix multiplication via the 3M and 4M methods. *ACM Trans. Math. Softw.*, 44(1):7:1–7:36, June 2017.
- [32] Field G. Van Zee, Tyler M. Smith, Bryan Marker, Tze Meng Low, Robert A. van de Geijn, Francisco D. Igual, Mikhail Smelyanskiy, Xianyi Zhang, Michael Kistler, Vernon Austel, John A. Gunnels, and Lee Killough. The BLIS framework: Experiments in portability. *ACM Trans. Math. Softw.*, 42(2):12:1–12:19, June 2016.
- [33] Field G. Van Zee and Robert A. van de Geijn. BLIS: A framework for rapidly instantiating BLAS functionality. *ACM Trans. Math. Softw.*, 41(3):14:1–14:33, June 2015.
- [34] <http://www.netlib.org/xblas>, 2019.
- [35] Chenhan D. Yu, Jianyu Huang, Woody Austin, Bo Xiao, and George Biros. Performance optimization for the k-nearest neighbors kernel on x86 architectures. In *Proceedings of the International Conference for High Performance Computing, Networking, Storage and Analysis, SC ’15*, pages 7:1–7:12, New York, NY, USA, 2015. ACM.

A Cascading a F64x2: Technical details.

How to cascade a given FP64x2 number into its four parts is conceptually easy, but requires care in practice so that it doesn't create unacceptable overhead.

Recall that cascading a number does not happen in isolation: All elements in a row of A or column of B must cascade conformally. Thus, we assume that $\sigma_0 = 2^e$ has been determined where e equals the exponent of the element with largest magnitude. The element we are cascading, $\widehat{\chi}$, is first scaled so that

$$\widehat{\chi} := \widehat{\chi} \times 2^{-e} = \pm \left[\begin{array}{|c|c|c|c|} \hline \beta_0 \cdots \beta_{D_0-1} & \beta_{D_0} \cdots \beta_{D_1-1} & \beta_{D_1} \cdots \beta_{D_2-1} & \beta_{D_2} \cdots \\ \hline \end{array} \right].$$

Here, as before, D_0 , D_1 , and D_2 indicate where splits occur, as illustrated with the boxes. If we are working with the element that is largest in magnitude, then $\beta_0 = 1$ and all digits starting with β_{2D} equal zero. Otherwise, there may be leading zero bits. The question now becomes how to extract the indicated parts into four FP64 numbers.

One way to achieve this is to recognize that ranges of the mantissa can be extracted by masking the corresponding bits and using a bit-wise logical AND operation. This allows one to extract χ_0 , χ_1 , and χ_2 , after which $\chi_3 = \widehat{\chi} - \chi_0 - \chi_1 - \chi_2$. The problem with this approach is that leading zeroes in sections may extract denormalized FP64 numbers and in the end FP64x2 subtraction is required to compute χ_3 . This results in an algorithm complicated by many conditionals, which in implementation incur considerable overhead. In other words, our experience is that this is slow.

We instead favor an approach that only computes with FP64 numbers, performance only FP64 arithmetic, and avoids all conditionals. We have found it to be fast enough.

The first observation is that, because the ranges of bits covered by χ_{hi} and χ_{lo} do not overlap, the two FP64 numbers that store $\widehat{\chi}$, χ_{hi} and χ_{lo} can be cascaded separately so that

$$\begin{aligned} \chi_{hi} &= \chi_{hi,0} + \chi_{hi,1}\sigma_1 + \chi_{hi,2}\sigma_2 + \chi_{hi,3}\sigma_3 \\ \chi_{lo} &= \chi_{lo,0} + \chi_{lo,1}\sigma_1 + \chi_{lo,2}\sigma_2 + \chi_{lo,3}\sigma_3. \end{aligned}$$

Then

$$\chi_i = \chi_{hi,i} + \chi_{lo,i}, \quad i \in \{0, 1, 2, 3\},$$

an addition that is exact when performed in FP64 arithmetic. This means we can focus on how to cascade a FP64 number, χ_\star where $\star \in \{hi, lo\}$, into four parts.

The second observation is that, given a FP64 number $\chi = \pm.\beta_0\beta_1 \cdots \beta_{D-1}\beta_D \cdots$ one can compute, in FP64 arithmetic, $\psi = \pm.\beta_0\beta_1 \cdots \beta_{d-1}$ via the steps

- $\psi := \chi$.
- $\psi = \psi + 2^{53-d} + 2^{53-d-1}$. Since the result is stored in a FP64 number, this removes bits starting with β_D .
- $\psi = \psi - 2^{53-d} - 2^{53-d-1}$.

(More precisely, this rounds to the first d digits. At least, if you get the details right and you take Greg's word for it!)

The third observation is that this computation will be performed for many FP64x2 numbers and hence various powers of two can be precomputed.

Putting all this together yields the following steps for cascading $\widehat{\chi}$, given that it needs to be scaled by 2^e :

- Consider $\widehat{\chi} = \chi_{hi} + \chi_{lo}$.
- $c_0 := D_0$, $c_1 := D_1 - D_0$, $c_2 := D_2 - D_1$
- for $\star \in \{hi, lo\}$:
 - Scale $\chi_\star = \chi_\star \times 2^{-e}$
 - $\chi_{\star,0} := \chi_\star$; $\chi_{\star,0} := \chi_{\star,0} + 2^{53-c_0} + 2^{53-c_0-1}$; $\chi_{\star,0} = \chi_{\star,0} - 2^{53-c_0} - 2^{53-c_0-1}$.
 - $\chi_\star := \chi_\star - \chi_{\star,0}$; $\chi_\star := \chi_\star \times 2^{c_0}$
 - $\chi_{\star,1} := \chi_\star$; $\chi_{\star,1} := \chi_{\star,1} + 2^{53-c_1} + 2^{53-c_1-1}$; $\chi_{\star,1} = \chi_{\star,1} - 2^{53-c_1} - 2^{53-c_1-1}$.
 - $\chi_\star := \chi_\star - \chi_{\star,1}$; $\chi_{\star,star} := \chi_\star \times 2^{c_1}$

- $\chi_{*,2} := \chi_*$; $\chi_{*,2} := \chi_{*,2} + 2^{53-c_2} + 2^{53-c_2-1}$; $\chi_{*,2} = \chi_{*,2} - 2^{53-c_2} - 2^{53-c_2-1}$.
- $\chi_{*,3} := \chi_* - \chi_{*,2}$; $\chi_{*,3} := \chi_{*,3} \times 2^{c_2}$.
- $\chi_i := \chi_{hi,i} + \chi_{lo,i}$ for $i = 0, 1, 2, 3$.

It is likely that many parts will equal zero because the active part of the FP64x2 number fall outside of range covered by the part.

A final observation is that because conditionals are avoided in the computation, cascading multiple FP64x2 numbers can be vectorized.